JOURNAL OF PLANKTON RESEARCH | VOLUME 32 | NUMBER 8 | PAGES 1105–1119 | 2010

Biovolume spectrum theories applied: spatial patterns of trophic levels within a mesozooplankton community at the polar front

SÜNNJE L. BASEDOW[1]*, KURT S. TANDE[1,2] AND MENG ZHOU[3]

[1]UNIVERSITY OF TROMSØ, 9037 TROMSØ, NORWAY, [2]BODØ UNIVERSITY COLLEGE, 8049 BODØ, NORWAY AND [3]DEPARTMENT OF ENVIRONMENT, EARTH AND OCEAN SCIENCES, UNIVERSITY OF MASSACHUSETTS, 100 MORRISSEY BLVD, BOSTON, MA 02125, USA

*CORRESPONDING AUTHOR: sunnje.basedow@uit.no

Received July 19, 2009; accepted in principle October 14, 2009; accepted for publication October 18, 2009

Corresponding editor: Roger Harris

Three-dimensional data on the mesoscale distribution of hydrography and mesozooplankton were collected at the Polar Front, northwestern Barents Sea, in spring 2008 (29 April–15 May) using a combination of multinet and towed instrument platform equipped with Laser Optical Plankton Counter, fluorometer and CTD. Trophic levels (TLs) within the zooplankton community (whole community and size-separated) were analysed for three consecutive periods using biovolume spectrum theory, which proved to be a powerful tool in the physically and biologically variable frontal system. Trophic structure was highly variable in time and across the Polar Front, but was mostly related to the phytoplankton bloom (as determined by fluorescence). High TLs of 5.5 within the zooplankton community were observed outside bloom situations (mostly in Atlantic Water) and were likely due to increased omnivory of *Calanus* spp., which dominated the large zooplankton size group that had a lower TL (2.2) during the bloom than outside blooms (max. TL 5.6). A strong input of herbivorous barnacle nauplii (Cirripedia) into the upper layer (35 000 ind. m^{-3} in net samples) substantially decreased mean TL in the marginal ice zone. Differences in TL estimates based on biovolume spectrum theory and other methods (stable isotopes, lipid markers, dietary analyses) are discussed.

INTRODUCTION

The development of biomass spectrum theories has given us a strong theoretical background to understand important processes within mesozooplankton communities based on semi-automatic sampling (Platt and Denman, 1978; Heath, 1995; Zhou and Huntley, 1997). Using time-sequences of measured zooplankton biomass spectra, it is possible to estimate *in situ* growth and mortality at the mesoscale (Silvert and Platt, 1978; Zhou and Huntley, 1997; Edvardsen *et al.*, 2002; Zhou *et al.*, 2004). The slope of a biomass spectrum provides the information on the trophic structure of a mesozooplankton community (Zhou, 2006). These mathematical theories and interpretations of biomass spectrum features allow us not only to observe the relationship between sizes and taxonomy, but also to understand the population and trophic dynamics.

Energy fluxes within aquatic systems determine the shape of the biomass spectrum (Platt and Denman,

doi:10.1093/plankt/fbp110, available online at www.plankt.oxfordjournals.org. Advance Access publication November 13, 2009

1978; Silvert and Platt, 1978; Sprules and Munawar, 1986; Heath, 1995; Zhou and Huntley, 1997; Zhou, 2006). Platt and Denman (Platt and Denman, 1977, 1978) described the energy flux through a given size interval as being governed mainly by individual growth within the size interval and by metabolism. Heath (Heath, 1995) characterized the flow of energy as a balance between individual and population growth on one side and mortality on the other side. Zhou and Huntley (Zhou and Huntley, 1997) unified both approaches and developed a mathematical theory of population dynamics that describes the energy flow through the biomass spectrum based on the distribution function of abundance and the law of the conservation of mass. The biomass spectrum theory developed by Zhou and Huntley (Zhou and Huntley, 1997) has thus a firm theoretical base and does not rely on any empirical assumptions, such as, for example, a constant predator–prey size ratio. Furthermore, the theory includes all sinks and sources that contribute to the flow of biomass through a given size interval. Recent research has pointed out the coherence between biomass spectrum theory and an individual-based model (IBM) (Law *et al.*, 2009), thereby further confirming biomass spectrum theory. The stochastic IBM was built starting from processes at the level of individuals and yielded a deterministic limit that was in close agreement to the partial differential equations of biomass spectrum theory (Law *et al.*, 2009).

Productive systems are characterized by a high intercept of the biomass spectrum. Enhanced primary production leads to an accumulation of biomass at small sizes and hence a high intercept (Zhou, 2006). In a time-varying system, accumulated biomass at small sizes can propagate along the biomass spectrum towards larger sizes. A high intercept of the biomass spectrum thus also denotes potentially higher secondary production. During a typical spring-bloom situation, for example, large amounts of phytoplankton biomass are transferred first to reproducing herbivores and then to developing mesozooplankton cohorts. These evolving mesozooplankton cohorts that feed and grow can be identified in the spectrum as waves propagating along the biomass spectrum (Silvert and Platt, 1978; Zhou and Huntley, 1997).

The slope of the biomass spectrum and the assimilation efficiency of the community provide information on the biomass recycling internally in the pelagic system, i.e. how many times biomass has been transferred from one pelagic organism to the next (Zhou, 2006). The slope of the biomass spectrum thus gives an instant picture of the pelagic system, but simultaneously contains information that was integrated in the system over time. A flat slope of the biomass spectrum indicates that the biomass has been recycled internally several times (Zhou, 2006). Trophic levels (TLs) computed by biomass spectrum theory can reach relatively high values in the plankton community because all fluxes are taken into account. This reflects the understanding today of the trophic coupling between phytoplankton, the microbial loop and mesozooplankton (Kirchmann, 2000; Fenchel, 2008). In a pelagic system where phytoplankton biomass is channelled via microzooplankton to copepods and back to detritus, microzooplankton and copepods, for example, the copepods have TL 6.

The number of trophic links between the microbial loop and the classic pelagic food web varies over short time scales. Trophic coupling is weakest during bloom periods when the most important mesozooplankton grazers feed nearly exclusively herbivorously (Levinsen *et al.*, 2000) and indeed have a low TL (Tamelander *et al.*, 2008). Outside the bloom, when the availability of phytoplankton is low and microzooplankton is relatively more abundant, mesozooplankton grazers have a more omnivorous diet (Levinsen *et al.*, 2000; Basedow and Tande, 2006) leading to an increase in TL (Tamelander *et al.*, 2008).

The Barents Sea is occupied by three main water masses: Arctic Water on the banks and in the northern Barents Sea, Atlantic Water in the deeper parts of the central Barents Sea and Coastal Water in the South along the Norwegian Coast (Loeng, 1991). The Polar Front, which separates Arctic from Atlantic Water, is thus associated not only with a change in salinity and water temperature but also with a gradient in bottom depth. At the front, mesoscale currents, meanders and eddies produce upwelling and vertical mixing of nutrients or enhance stratification. This leads to enhanced short-term primary production at the mesoscale, and strong gradients of plankton communities. During spring, the retreating ice-edge is found in close vicinity to the Polar Front. The abiotic environment thus differs greatly over small spatial scales, making it challenging to sample the frontal system adequately. The high inter-annual and local variability in the development of the phytoplankton bloom in the marginal ice zone further increases sampling complexity (Engelsen *et al.*, 2002; Reigstad *et al.*, 2002).

Our aim was to analyse the impact of mesoscale physical processes on food web dynamics within the plankton community at the Polar Front during spring 2008. We sampled the frontal area using a combination of semi-automatic high-resolution mapping and detailed analyses at stations. Applying biovolume spectrum theories to the data, we investigated differences between water masses in the trophic structure of the zooplankton community in the northwestern Barents Sea.

METHOD

Field sampling

The Polar Front in the Barents Sea meanders along topography and separates Atlantic Water from colder, less saline Arctic Water (Loeng, 1991). In an area of the Polar Front southeast of Hopen Island (Fig. 1), data on the spatial and temporal distributions of hydrography and mesozooplankton were collected during the IPY-NESSAR project in spring 2008 (29 April–2 May and 9–14 May). For data collection, a towed instrument platform (Scanfish; GMI, Denmark) was equipped with a Laser Optical Plankton Counter (LOPC; Brooke Ocean Technology Ltd, Canada), a CTD (SBE 911plus, Seabird Electronics Inc., USA) and a fluorometer (F; Seapoint Chlorophyll Fluorometer, Seapoint Sensors Inc., USA). The Scanfish undulated between surface and 75 m (or between surface and 15 m above bottom depth if bottom depth was below 90 m) while it was towed along transects (Fig. 1) at a speed of 6–7 knots. Each tow of the Scanfish lasted for 2–3 days during which LOPC-CTD-F data were logged continuously (2 Hz). Before and after the tows, CTD profiles and discrete water and zooplankton net samples (Multinet, 180 μm mesh width, 0.25 m^2 mouth opening) were collected at 12 stations in the study area to compare with and interpret the LOPC-CTD-F data (Table I). The depth layers sampled by multinet (vertical tows) were chosen based on hydrography and fluorescence profiles at each station to facilitate data interpretation.

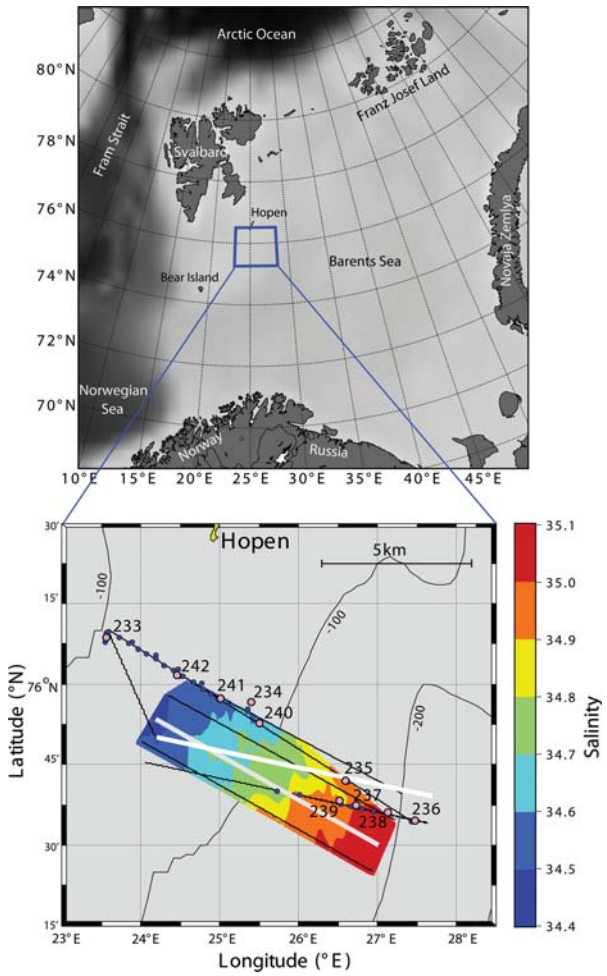

Fig. 1. Study area. The location of the study area within the Barents Sea is marked with a blue square in the upper map. The lower map shows the transects sampled with the Scanfish-instrument-package (black lines), CTD stations (blue circles) and multinet stations (pink circles, numbered). The transects shown in Figs 2 and 3 are highlighted in grey (1 May) and white (10 and 14 May), respectively. The salinity (interpolated data between 20 and 30 m, see Method) is shown to depict the location of the Polar Front (34.8–35.0).

Analyses of samples and LOPC data

Zooplankton samples were preserved in a solution of 20% fixation agent (50% formalin buffered with hexamine, 50% anti-bactericide propandiol) and 80% seawater. In the laboratory, zooplankton was counted and identified to species and stage or to the lowest taxonomical level feasible under a stereo-microscope. *Calanus finmarchicus* and *Calanus glacialis* as well as the younger stages of *Calanus hyperboreus* were distinguished by size (Daase and Eiane, 2007). Abundance was calculated based on filtered volume obtained from the flow meters attached to the multinet.

The LOPC was designed to overcome some of the problems associated with the OPC, it counts and measures particles that pass through a laser beam inside the instrument as the LOPC moves through the water (Herman *et al.*, 2004). The size of particles is returned as digital size, which can be converted into equivalent spherical diameter (ESD), a quantity that yields the diameter that a particle had if it were an opaque sphere. ESD is thus a property describing the size as well as the transparency of a particle. We calculated the ESD as described in Gaardsted *et al.* (Gaardsted *et al.*, in review). LOPC data were analysed using the python programming language (version 2.6.2) and basically following the instructions in the LOPC manual (Anonymous, 2006). The LOPC detects living and dead particles in the size range of ca. 0.1–35 mm ESD (Herman *et al.*, 2004). Major non-living particles in the water column are marine snow and phytoplankton aggregates. As discussed at length in Edvardsen *et al.* (Edvardsen *et al.*, 2002), marine snow and phytoplankton aggregates >0.1 mm are very likely eroded when towing an OPC at 6 knots because of micro-scale

Table I: Stations in the study area (Fig. 1) at the Polar Front East of Hopen Island, Barents Sea, where the multinet was deployed in spring 2008

Station	Latitude (°N)	Longitude (°E)	Date	Time (UTC)	Echo-depth (m)	Sampling interval (m)
228	75 45.44	26 35.46	29 April	22:10	139	125–90–60–30–0
229	75 49.78	26 01.19	30 April	03:55	118	100–40–25–0
230	75 58.16	24 59.73	30 April	08:15	116	60–30–0
231	76 03.18	24 18.96	30 April	12:55	75	60–30–0
233	76 08.66	23 33.82	9 May	07:33	50	40–20–0
234	75 56.75	25 24.13	9 May	16:25	114	100–60–25–2
235	75 42.05	26 35.81	9 May	21:15	133	120–50–25–2
236	75 34.62	27 28.38	10 May	02:52	167	240–100–50–25–1
238	75 36.20	27 08.33	12 May	09:42	225	200–170–150–110–60–0
239	75 38.19	26 30.85	12 May	14:25	132	100–60–35–10–1
240	75 52.81	25 30.27	12 May	18:50	105	90–70–55–35–1
242	76 01.80	24 27.18	13 May	01:50	70	50–30–10–2

Station numbers, latitude, longitude, date, time, depth of the station and sampling depths of the multinet are given.

turbulence and associated shear stress at the opening of the OPC and there is no reason to believe that shear stress should be less at the opening of the LOPC. Therefore, though we cannot completely rule out that some phytoplankton aggregates might have been counted, we are assured that the majority of particles counted by the LOPC in this study were zooplankton particles. For each individual zooplankton particle, body volume was computed from its ESD. For biovolume spectra analyses, data were then grouped into 50 size groups of equal (body volume) increments to increase statistics and to clarify data presentation.

The ESD of all zooplankton genera that were abundant in net samples was estimated either based on literature concerning the OPC (Edvardsen *et al.*, 2002; Basedow *et al.*, 2008) or, for genera for which no literature data exist, estimated based on the ESD of similar sized genera. For data interpretation and presentation (Fig. 3), the data collected by LOPC were then divided into four size groups: S, M, L and XL (Table III). To our knowledge, no data on the calibration of the LOPC for northern marine plankton in spring/summer exist; therefore, we chose relatively coarse size ranges, each of which incorporates different species and stages. Particles <0.25 mm ESD were not included into our analyses because very small particles that result from the erosion of phytoplankton aggregates and marine snow would fall into this group and would corrupt our analyses. Few animals >5.5 mm were observed in Arctic and Polar Front Water and none in Atlantic Water. The XL size group thus consisted mostly of particles between 2 and 5.5 mm ESD.

Preparation of figures

Data on hydrography and zooplankton distribution are presented from selected transects (Figs 2 and 3). These figures were prepared by gridding and interpolating all data points collected along the transects. For interpolation, we used the natural neighbour interpolation that is built in pythons matplotlib library. The salinity plot overlaid onto the map (Fig. 1) was prepared much the same way, the only difference being that data points between 20 and 30 m from all transects were interpolated. All other figures were also prepared using the matplotlib library (version 0.98.5.2) (Hunter, 2007) in python. To simplify data presentation and aid comparison with LOPC data, abundance data obtained from Multinet are presented from the upper layer (0–ca. 60 m) and lower layer (ca. 60 m–bottom) in Table II and Fig. 4. The division at ca. 60 m was chosen because net samples were obtained from above and below 60 m at most stations (Table I) and because 0–60 m is close to the 0–75 m depth layer that was sampled by the LOPC.

Biovolume spectra analyses

Biovolume spectra are analogue to biomass spectra and are used if only the size and no weight of individuals is available (Edvardsen *et al.*, 2002; Quinones *et al.*, 2003; Zhou *et al.*, 2004). The normalized biovolume spectrum b (Platt and Denman, 1978; Zhou and Huntley, 1997; Edvardsen *et al.*, 2002) is defined as

$$b = \frac{\text{biovolume in size interval } \Delta w}{\text{size interval } \Delta w \,(\text{in m}^{-3})} \qquad (1)$$

with w being the body volume of an individual zooplankton in cubic millimetre. We computed the biovolume spectra for each of the three sampling times (30 April–2 May, 10–12 May, 14–15 May) and each of the three water masses (Arctic Water, Polar Front Water, Atlantic Water) separately in order to analyse differences

Table II: Composition of the mesozooplankton community at the Polar Front East of Hopen Island, Barents Sea, in spring 2008

	Station																		
	228		229		230	231	233	234		235		236		238		239		240		242
Species/group	UL	LL	UL	LL	UL	UL	UL	UL	LL	UL	LL	UL	LL	UL	LL	UL	LL	UL	LL	UL
Polychaeta larvae	0.3	—	1.6	0.2	12.1	85.3	172	48.1	—	1.4	0.3	—	—	—	—	14	0.3	18	3.7	81.6
Eggs unidentified	3.7	22.7	52.2	1.9	2594.8	10.7	6	1466.8	48.4	83.3	32.2	3.6	1.9	0.5	11.6	507.2	13.1	806	129.8	3389.5
Cirripedia nauplii	0.6	3.3	49.1	—	10 820.8	34 928	10 802.3	214.1	86	303.1	53.9	1.1	0.1	0	0.4	201.8	2.1	472	15.3	5058.7
Copepoda																				
Calanus nauplii	5.9	0.8	4.9	0.1	14.1	4.7	2	21.7	—	5.9	3.1	1.5	3.9	5	9.6	175.3	1.5	106	5.7	256.2
C. finmarchicus CI–CIII	—	0.1	—	—	0.4	0.7	—	—	—	—	—	—	—	0.3	0.3	1.8	0.2	—	—	—
C. finmarchicus CIV–CVI	0.3	11.9	0.9	0.7	6.6	29.8	25.1	7.6	2.9	0.8	3.4	0.2	0.7	0.1	18	0.5	1.1	2.4	6.2	20.5
C. glacialis CI–CIII	—	0.1	0.1	0.2	0.1	0.7	3.1	0.5	0.8	—	—	—	—	0.1	—	7.3	0.1	0.5	0.5	2.5
C. glacialis CIV–CVI	—	2	—	0.2	30.2	10	5.5	7.6	5.8	0.1	0.4	—	0.1	—	1.7	—	0.2	0.2	5.2	13.5
Metridia longa	—	3.4	—	—	—	0.8	–	0.1	2	0.1	0.7	0.8	0.9	0.1	1.6	—	—	3	—	1.7
Pseudocalanus spp.	0.7	16.8	3.3	2.5	47.7	138.7	331	13.3	12.8	8.6	18.3	0.3	0.7	0.1	6.7	1	4.3	1	28	40.9
Microcalanus spp.	1.1	4.9	0.3	0.7	0.4	13.3	27.7	6.1	56.8	4.9	19.3	0.2	3.5	0.1	44.8	2.1	3.8	7	100.8	24.2
Oithona similis	7	15.7	12	3.5	14.8	19.3	18.4	191.1	9.2	15.4	21	3.9	5.4	3.9	26.6	60.7	77.8	43	17.2	61.9
Oithona atlantica	—	0.3	—	—	—	—	—	0.5	—	—	—	—	0.1	—	1.1	0.3	0.4	0.1	—	—
Oncaea borealis	—	—	—	—	—	—	—	1.6	0.8	0.2	—	—	—	—	—	2	0.1	2	1.5	5.9
Thysanoessa inermis	—	—	—	—	—	—	—	0.3	—	—	0.1	—	—	—	—	—	—	0.2	1	0.1
T. longicaudata	—	0.1	—	—	—	—	—	0.1	—	—	0.2	—	—	—	—	—	—	0.2	0.7	—
Krill nauplii	—	—	—	—	—	—	—	99.5	0.2	—	0.1	—	—	—	—	25.8	—	68.2	4.5	114.5
Amphipoda	—	—	0.1	—	—	1	0.3	—	—	—	—	—	—	—	—	0.2	—	0.6	—	1.1
Chaetognatha	0.1	0.3	—	—	—	1.2	0.6	1.1	0.1	0.1	0.7	—	0.1	—	—	—	—	2.1	1.3	1.8
Hydrozoa	0.2	0.1	—	—	—	0.5	0.4	0.5	—	0.1	—	—	—	—	—	—	—	—	—	—
Ctenophora	0.1	0.7	0.4	0.2	—	0.3	0.4	0.6	0.5	0.3	—	0.6	—	0.1	—	0.7	0.5	0.5	0.7	0.4
Fish larvae	—	—	—	—	—	—	—	—	—	0.1	—	—	—	0.1	—	—	—	—	—	—

Abundance obtained from multinet samples is given as individuals per cubic metre for the upper layer (0–60 m, UL) and lower layer (60 m–bottom, LL) at each station.

Table III: Classification of size groups applied to the LOPC data and the most important zooplankton groups in the small (S), medium (M), large (L) and extra large (XL) size group

	ESD (mm)	Most important zooplankton groups in size range
S	0.25–0.6	*Balanus* nauplii, eggs, *Oithona* spp., *Calanus* nauplii, *Microcalanus*
M	0.6–1	*Pseudocalanus* spp., *Metridia longa*
L	1–2	*Calanus* spp. CIV, CV, adult (juvenile krill?)
XL	2–14	*Thysanoessa* spp.

LOPC data were collected along transects crossing the Polar Front East of Hopen Island, Barents Sea, in spring 2008 (Fig. 1).

in time and between water masses. To compare the spectra with each other, the slope of the observed biovolume spectra was calculated by fitting (least-squares) a linear function to each spectrum. For each biovolume spectrum, one slope was fitted to the whole size range and four to each of the size ranges of the four zooplankton groups S, M, L and XL (Table III). Because the LOPC measured few particles >5.5 mm ESD, the slope for the XL size group was fitted to the biovolume spectrum between 2.0 and 5.5 mm ESD only. On the basis of the slope of the biovolume spectrum and the mean assimilation efficiency of zooplankton (η_n), we estimated the number of TLs within the zooplankton community (Zhou, 2006):

$$\mathrm{TL} = \frac{-(1+\eta_n)}{(\delta \ln b / \delta \ln w)} \qquad (2)$$

In contrast to general biomass spectrum theory, which does not depend on any empirical assumptions, the computation of TLs is based on the assumption that the biovolume spectrum can be linearized on a logarithmic scale (Zhou, 2006). Furthermore, the assimilation efficiency of the zooplankton community has to be known to calculate TLs (Zhou, 2006). We applied a mean assimilation efficiency of 70%, a value commonly used for copepods. Data on assimilation efficiency in zooplankton are limited, and the existing data show a great variability depending on food source and species (Mauchline, 1998). For *Pseudocalanus* spp., mean assimilation efficiency may be lower than 70%, values reported range from 10% to 71% (Harris and Paffenhöfer, 1976; Corkett and McLaren, 1978; Koski *et al.*, 1998), whereas for carnivores assimilation efficiency may be as high as 98% (Mauchline, 1998). TL estimates do not depend strongly on assimilation efficiency (Zhou, 2006, their Fig. 2), assuming a slope of the biovolume spectrum of −1.5, for example, and changing the assimilation efficiency from 70% to 50%, the estimated TL would increase from 1.6 to 2.0 [Equation (2)]. We therefore chose to hold assimilation efficiency constant with size. Thus, though the estimated TLs may not represent exact TLs, the variations of TL represent the differences in trophic structure between plankton communities. To analyse food web dynamics within the zooplankton community, we first estimated the number of TLs within the whole zooplankton community (size groups S to XL). We then estimated the number of TLs within those size groups for which a significant slope could be fitted to the biovolume spectra.

RESULTS

Hydrography and fluorescence

We worked in the frontal area and most of our study area was occupied by Polar Front Water with a salinity between 34.8 and 35.0 (Loeng, 1991). Polar Front Water was mainly found between the 150 and 200 m isobaths. Arctic Water with a salinity between 34.3 and 34.8 occupied the shelf in the western part and Atlantic Water with a salinity >35.0 was found in the very East of the study area (Figs 1 and 2, top panel). Temperatures were around −1°C in Arctic Water and around 3°C in Atlantic Water and they remained relatively stable throughout the 2 weeks (Fig. 2, middle panels). The westernmost stations in Arctic Water were close to the ice edge where the stratification of the water column had started, while the water column in Atlantic Water was still well mixed (Fig. 2) down to the bottom (CTD data, not shown).

On 1 May, fluorescence was highest in Arctic Water close to the ice edge. On 10 May, highest values were still found in Arctic Water but farther west and on 14 May highest fluorescence values had increased by one order of magnitude and were now observed in Polar Front Water in the centre of the study area (Fig. 2, lower panels). In Atlantic Water, very low fluorescence was observed throughout most of the study area (Fig. 2), only at the southeastern-most corner were fluorescence values slightly elevated at the end of the study (values around 1, data not shown).

Zooplankton community

In general, abundances of all mesozooplankton groups ranged from low to very low in Atlantic Water, whereas those in Polar Front Water and in Arctic Water were relatively high (Table II, Fig. 3). The zooplankton community in Arctic Water on the shelf was completely

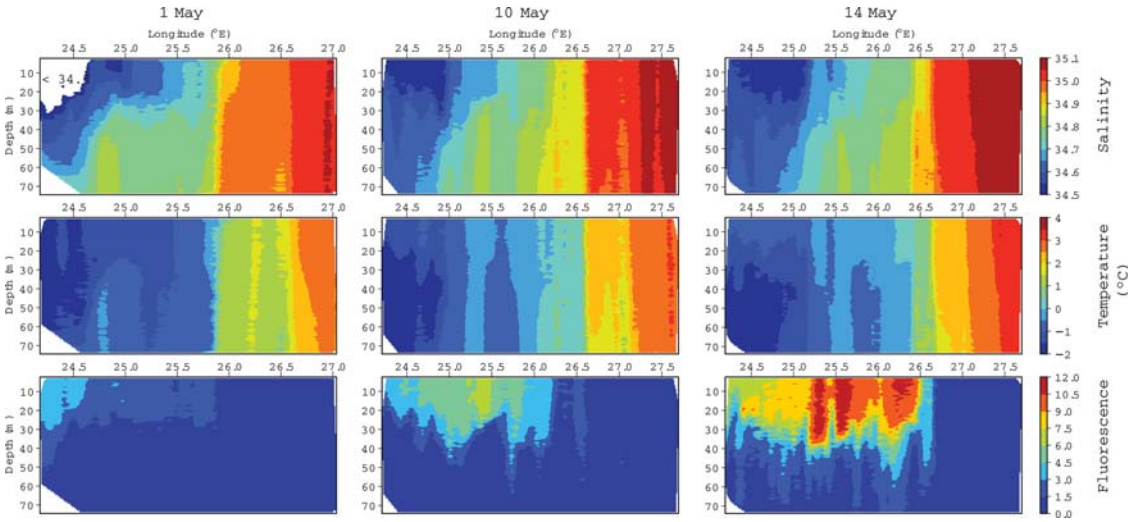

Fig. 2. Salinity (top), temperature (middle) and fluorescence (down) along transects crossing the Polar Front in the Barents Sea East of Hopen Island during 1 May (left), 10 May (centre) and 14 May (right) 2008. The figure is based on data sampled by a CTD that was towed on an instrument platform. For location of transects refer to Fig. 1.

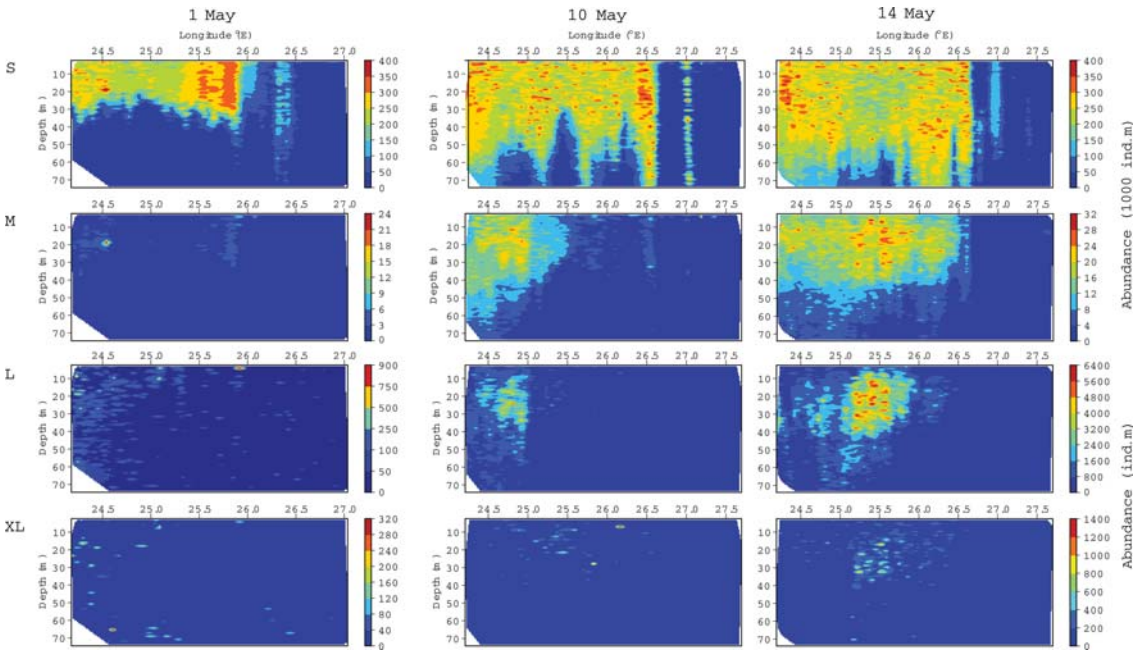

Fig. 3. The distribution of different zooplankton size groups along transects crossing the Polar Front East of Hopen Island in the Barents Sea, May 2008. First row: Distribution of small zooplankton (S), second row: medium zooplankton (M), third row: large zooplankton (L), fourth row: extra large zooplankton (XL). The division of the size groups is given in Table III and the location of the transects can be seen in Fig. 1. Note the different scale in the top most panels compared with the two lower panels, as well as the different scales on 1 May and 10 and 14 May, respectively. The figure is based on data collected by an LOPC that was towed on an instrument platform.

dominated by meroplanktonic larvae (Fig. 4) and especially by barnacle larvae, which reached extremely high abundances of up to 35 000 ind. m^{-3} (Table II). Also unidentified eggs (0.2–0.4 mm) were abundant in Arctic Water (Table II, Fig. 4). Barnacle larvae and unidentified eggs were also abundant in Polar Front Water on the shelf, but were mostly absent in deeper areas and in Atlantic Water (Table II). The distribution of small copepods (*Oithona* spp., *Microcalanus*) did not follow any obvious pattern in relation to water masses or depth (Table II); however, they were more important below 60 m, where eggs and larvae were comparatively rare (Fig. 4). Abundances of small zooplankton measured by LOPC (S size group) revealed maximum

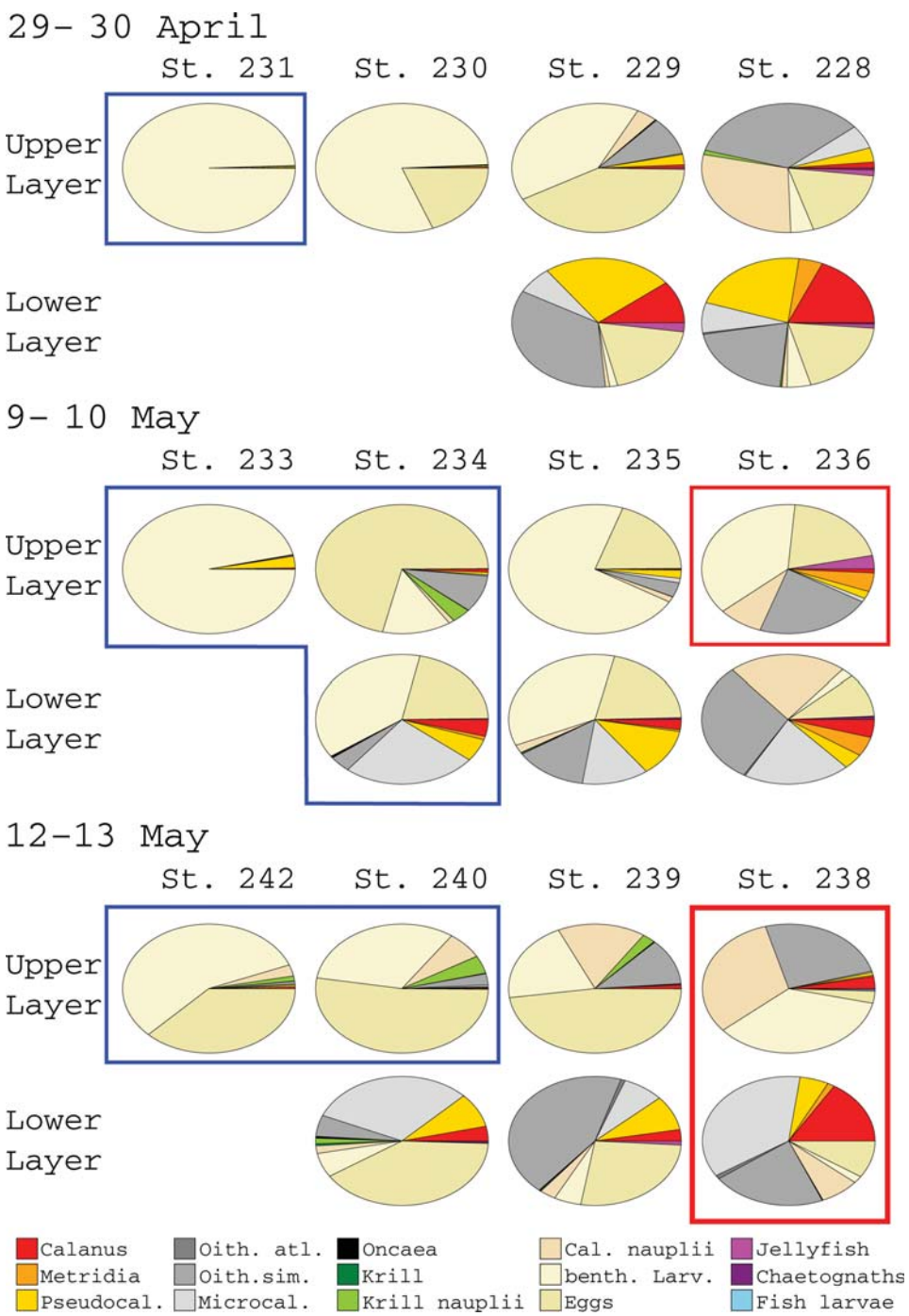

Fig. 4. The relative importance of different zooplankton species or groups at 12 different stations in Arctic Water (stations marked with a blue square), Polar Front Water (stations not marked) and Atlantic Water (red square). Stations were located in the Barents Sea at the Polar Front East of Hopen Island (Fig. 1) and were sampled by Multinet in spring 2008. At each station, the proportion of species/groups in the upper layer (0–60 m) and lower layer (60 m–bottom), respectively, is shown. Calanus, *Calanus finmarchicus*+*Calanus glacialis*; Metridia, *Metridia longa*; Pseudocal., *Pseudocalanus* spp.; Oith. atl., *Oithona atlantica*; Oith. sim., *Oithona similis*; Microcal., *Microcalanus* spp.; Oncaea, *Oncaea borealis*; Krill and Krill nauplii, *Thysanoessa longicaudata*+*Thysanoessa inermis* and naupliar stages of these; Cal. nauplii, *Calanus* spp. nauplii; benth. Larv., meroplanktic larvae; Eggs, unidentified eggs (0.2–0.4 mm); Jellyfish, Hydrozoa+Ctenophora; Chaetognaths, *Sagitta* spp.+*Eukrohnia* sp.

abundances of 400 000 ind. m^{-3}, i.e. one order of magnitude higher than measured by multinet (Fig. 3, first row). The mesoscale pattern of the distribution of small zooplankton was closely linked to areas with high fluorescence. At a small scale, however, small zooplankton was more patchily distributed than fluorescence (Figs 2 and 3).

Of the medium sized-copepods, *Pseudocalanus* spp. was most abundant; highest abundances (100–330 ind. m^{-3}) were found in Arctic Water, but also in Polar Front Water *Pseudocalanus* spp. was important (Table II). Again, during the first sampling, abundances of the medium size group (M) measured by LOPC were one order of magnitude higher than abundances measured by multinet (Table II; Fig. 3, second row). Later on, during the second and third sampling in mid-May, abundances of medium-sized zooplankton had increased to around 10 000–25 000 ind. m^{-3} in Arctic Water and Polar Front Water. From these areas, unfortunately, no net samples from mid-May are available to directly compare with the LOPC.

The larger copepods *C. glacialis* and *C. finmarchicus* occurred as nauplii, older copepodites (CIV–V and some few CIII) and adults in the study area (Table II). Both *Calanus* species were observed in Arctic Water on the shelf (Table II) where they were reproducing (own observation), and where nauplii were most abundant at the end of our study (Table II). *Calanus finmarchicus* was also found at depths (>150 m) in Atlantic Water and in Polar Front Water (Table II, Fig. 4) but was in diapause there (own observation). The LOPC measured abundances of mostly between 100 and 250 ind. m^{-3} during 1 May (Fig. 3, third row left), i.e. ca. three to five times higher than abundances obtained from multinet (Table II). Large zooplankton occurred mostly in small-scale patches in Arctic Water and in Polar Front Water (Fig. 3). High abundances of about 4000 ind. m^{-3} were observed in a larger patch in Polar Front Water during 14 May (Fig. 3, third row right). The patch measured ca. 1.5 km along the transect and stretched from 10 to 40 m depth.

The krill species *Thysanoessa inermis* and *Thysanoessa longicaudata* were caught by multinet in Polar Front Water and in Arctic Water; however, samples yielded low abundances and only krill nauplii were more abundant (Table II). Neither nauplii nor older krill were caught during the first sampling at the end of April. The LOPC measured small-scale patches of zooplankton in the size range of krill (XL size group) in Polar Front Water and in Arctic Water during all three sampling periods (Fig. 3, fourth row). During 14 May, in Polar Front Water, a patch was observed that sharply ended at the border between Polar Front Water and Arctic Water (Fig. 3, fourth row right). Abundances of XL zooplankton were mostly around 500 ind. m^{-3} but maximum values of 1400 were reached locally (Fig. 3, fourth row).

Biovolume spectra and trophic levels

The biovolume spectra from Arctic Water had a higher intercept than the spectra from Polar Front Water and these again had a higher intercept than those from Atlantic Water (Fig. 5, upper panel), reflecting the observed high abundances in Arctic Water and very low abundances in Atlantic Water (Fig. 3). In all three water masses, the intercepts of the biovolume spectra increased with time (Fig. 5), indicating an increase in production in the frontal system over time.

In Arctic Water, the biovolume spectrum became flatter in the course of the two sampling weeks (Fig. 5, upper panel left). The slope that was fitted to the biovolume spectra of the whole zooplankton community thus decreased (Fig. 5, lower panel left; Table IV), and TLs in the community increased from 3.6 at the end of April to 5.5 in the mid of May (Table V). A flattening of the spectra and an increase in TLs were also observed in Polar Front Water (Fig. 5, centre), though the increase in TLs was not as pronounced as in Arctic Water (Table V). In Atlantic Water, the opposite pattern was observed: in mid-May the slope of the biovolume spectrum was steeper than at the end of April (Fig. 5, bottom right; Table IV). The zooplankton community in Atlantic Water was thus characterized by more TLs in the beginning of the study than at the end (Table V).

In all water masses, the TL of medium-sized zooplankton was around 1 at the end of April (Table V); these very low TLs may indicate that medium-sized zooplankton in the upper layer was feeding purely herbivorously during that time. In Arctic Water, TL within the medium-sized zooplankton group increased to 4.7 on 10 May, while the increase in Polar Front Water was more moderate to 1.3 on 10 May and 2.2 in the mid of May (Table V). In Atlantic Water, medium-sized zooplankton had a TL of ~1 during the whole sampling period, though it was a little higher during the second sampling (Table V).

Within the large zooplankton group, TL increased in Arctic Water during the course of sampling, reaching a TL of 4.4 in the mid of May (Table V). In contrast, in Polar Front Water, TL of large zooplankton was high (5.5) at the end of April and gradually decreased towards mid-May (Table V). A similar pattern was observed in Atlantic Water, where the large size group had a high TL of 5.6 during the second sampling and a lower TL of 2.9 during the third sampling (Table V).

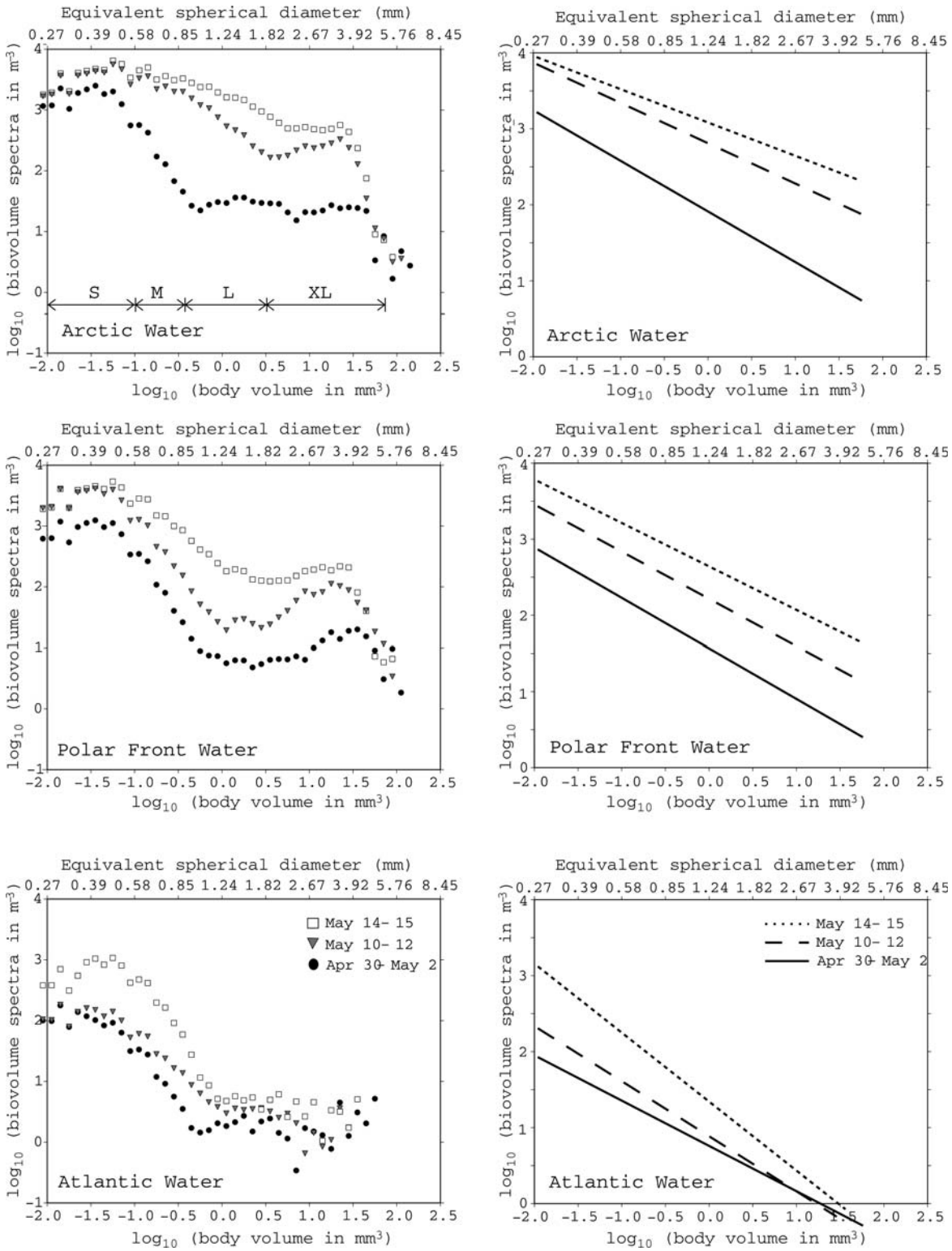

Fig. 5. Biovolume spectra (top) of the zooplankton community in spring 2008 at the Polar Front east of Hopen Island, Barents Sea, and the associated slopes to each spectrum (bottom). Spectra were computed based on data collected by a towed LOPC (see Method) and are shown for the community in Arctic Water (left), Polar Front Water (centre) and Atlantic Water (right). For each water mass, the spectra from the three sampling periods (30 April–2 May, 10–12 May, 14–15 May) are displayed.

Table IV: Parameters of the linear functions fitted to the biovolume spectra, which were obtained from LOPC data collected at the Polar Front East of Hopen Island, Barents Sea (Fig. 5), from Arctic, Polar Front and Atlantic Water, respectively, for the three sampling periods

Water mass	Time	Size group	Intercept	Slope	*r*	*P*-value
Arctic Water	30 April–2 May	S	2.88	−0.21	0.09	0.39
		M	0.59	−2.28	0.98	<0.001
		L	1.47	0.15	0.42	0.06
		XL	1.62	−0.28	0.20	0.13
		All	1.91	−0.67	0.80	<0.001
	10–12 May	S	3.97	0.29	0.28	0.12
		M	3.04	−0.52	0.77	0.02
		L	2.81	−1.11	0.99	<0.001
		XL	2.84	−0.58	0.29	0.06
		All	2.81	−0.53	0.82	<0.001
	14–15 May	S	4.13	0.36	0.40	0.048
		M	3.32	−0.35	0.58	0.08
		L	3.26	−0.56	0.97	<0.001
		XL	3.6	−0.96	0.51	0.006
		All	3.08	−0.44	0.71	<0.001
Polar Front Water	30 April–2 May	S	2.71	-0.14	0.05	0.53
		M	0.35	−2.34	0.98	<0.001
		L	0.86	−0.44	0.77	0.002
		XL	0.59	0.38	0.57	0.003
		All	1.57	−0.66	0.68	<0.001
	10–12 May	S	3.29	-0.11	0.04	0.59
		M	1.30	−1.9	0.98	<0.001
		L	1.53	−0.59	0.64	0.0096
		XL	1.65	0.07	0.01	0.72
		All	2.22	−0.62	0.68	<0.001
	14–15 May	S	3.81	0.18	0.12	0.32
		M	2.41	−1.12	0.94	0.0013
		L	2.41	−0.79	0.94	<0.001
		XL	2.69	−0.56	0.28	0.06
		All	2.64	−0.57	0.83	<0.001
Atlantic Water	30 April–2 May	S	1.23	−0.48	0.51	0.02
		M	-0.36	−2.02	0.98	<0.001
		L	0.26	0.16	0.24	0.18
		XL	−0.21	0.37	0.21	0.11
		All	0.76	−0.59	0.71	<0.001
	10–12 May	S	1.75	−0.21	0.16	0.26
		M	0.48	−1.39	0.96	<0.001
		L	0.65	−0.43	0.61	0.013
		XL	0.5	−0.26	0.09	0.38
		All	0.89	−0.72	0.91	<0.001
	14–15 May	S	3.18	0.25	0.15	0.26
		M	0.93	−1.88	0.98	<0.001
		L	0.88	−0.84	0.71	0.004
		XL	0.76	−0.23	0.11	0.31
		All	1.34	−0.91	0.86	<0.001

Table V: TLs of the zooplankton community East of Hopen Island, Barents Sea, in spring 2008 in Arctic, Polar Front and Atlantic Water, respectively

		Sampling period		
Size group	Water mass	30 April–2 May	10–12 May	14–15 May
All	Arctic Water	3.6	4.6	5.5
	Polar Front Water	3.7	3.9	4.3
	Atlantic Water	4.1	3.4	2.7
M	Arctic Water	1.1	4.7	NS
	Polar Front Water	1.0	1.3	2.2
	Atlantic Water	1.2	1.8	1.3
L	Arctic Water	NS	2.2	4.4
	Polar Front Water	5.5	4.1	3.1
	Atlantic Water	NS	5.6	2

TLs were computed from the slope (Table IV) of the biovolume spectra (Fig. 5) for medium-sized zooplankton (M), large zooplankton (L) and the whole community (all) if slopes where significant. NS, not significant. Refer to Table III for an overview of the most important zooplankton groups in each size class.

DISCUSSION

The surface manifestation of the Polar Front and its associated physical and biological features southeast of Hopen Island in the Barents Sea were well resolved by our sampling strategy. The data showed a small-scale variability of nearly all measured parameters along transects. This stresses the importance of adequate high-resolution sampling in order to capture a true picture of the frontal system.

High fluorescence values proceeded from Arctic Water, which had recently become ice-free, towards Polar Front Water following stratification of the water column during the 2 weeks of our study. During spring, the phytoplankton bloom in the Barents Sea is dominated by chlorophyll-rich species (Rey *et al.*, 1987; von Quillfeldt, 2000; Hodal and Kristiansen, 2008) and fluorescence is then a good indicator of phytoplankton (Signorini and McClain, 2009). In polar ecosystems, the bloom often progresses from the ice edge and early-stabilized Arctic Water towards well-mixed open water (Rey and Loeng, 1985; Waniek *et al.*, 2005). We can therefore be reasonably sure that we encountered a phytoplankton bloom that proceeded from Arctic Water towards Polar Front Water in the course of our study. In the Barents Sea, blooms in Atlantic Water might appear with increased solar radiation in unstratified water columns (Eilertsen, 1993) as late as June (Wassmann *et al.*, 1999). In our case, Atlantic Water remained in a winter situation throughout the sampling period in large parts, but not in the southeastern-most corner of the study area. Accordingly, the zooplankton community in Arctic Water corresponded to a spring situation with high abundances of larval stages, whereas the Atlantic community corresponded mostly to a winter situation with generally lower mesozooplankton abundances and *Calanus* sp. being located in diapause at depth.

The abundance of small (0.25–0.6 mm ESD) and medium (0.6–1.0 mm ESD) particles measured by LOPC was about one magnitude higher than that in the same size range observed in multinet samples (180 μm mesh width). This is in line with recent analyses estimating that <10% of zooplankton <0.8 mm length is retained by a 200 μm net (Gallienne and Robins, 2001), and it is also consistent with earlier studies showing that a significant proportion of copepods is lost if sampled with a mesh width larger than 75% of their body width (Nichols and Thompson, 1991). Locally, the LOPC also measured higher abundances of large zooplankton (1–2 mm ESD) than those observed from multinet samples. This contradicts findings showing that abundances of older stages of *Calanus* sp. are comparable, measured either by multinet or by LOPC (Gaardsted *et al.*, in review). On the basis of the patchy distribution of large zooplankton (Fig. 3), we suppose that we missed the patches of high abundances of *Calanus* spp. with our net sampling in Arctic Water. We cannot rule out, however, that the large size group also contained some juvenile krill and this may indeed have been the case in Polar Front Water on 14 May (Fig. 3, third row right). In general, the multinet is not geared towards catching larger, more motile species (Sameoto *et al.*, 2000), it was therefore not unexpected that the LOPC, with a higher towing speed, indicated higher abundances of krill (extra large size group, 2–14 mm ESD) compared with abundances of *Thysanoessa* spp. obtained from multinet samples. To conclude, in all probability, the LOPC was more reliable in capturing true abundances of all size groups in the upper 75 m than the multinet.

The abundances of *Balanus* sp. nauplii observed in Arctic shelf waters and in Polar Front Water were up to 35 000 ind. m^{-3} in net samples. These high abundances are comparable to abundances of barnacle nauplii observed in the Western Atlantic off Rhode Island during peak spawning (Lang and Ackenhusen-Johns, 1981), and to abundances observed in May on the shelf north of Svalbard (Blachowiak-Samolyk *et al.*, 2007), and thus indicate that peak spawning of *Balanus* sp. was taking place during our survey period. The input of biomass from the benthic community into the upper layer was clearly visible in the biovolume spectra. In Arctic Water and in Polar Front Water, the pronounced increases of the biovolume spectra observed in the size range of small zooplankton from the end of April to 10–12 May and from 10–12 May to 14 May exceeded any potential increases associated with body and population increases internally within the community. This indicates that external biomass had to be supplied into the upper layer and highlights the importance of benthic–pelagic coupling during spring on the Arctic shelf. In Atlantic Water, the increase in the biovolume spectrum in the size range of small zooplankton was most pronounced from 10–12 May to 14–15 May, indicating that barnacle nauplii reached the upper layer later here. It is not clear from our data if barnacle nauplii were released in Atlantic Water or if they were advected from the Arctic shelf into Atlantic Water.

The intercepts of the biovolume spectra in Arctic and Polar Front Water were high, compared with the few biovolume spectra that exist in the literature. Intercepts were comparable to the spectra obtained from a fjord in northern Norway in May/June (Edvardsen *et al.*, 2002) but higher than observed in a highly productive region offshelf the Norwegian coast in May/June (Zhou *et al.*, 2009). The biovolume spectra from Arctic and Polar Front Water thus indicate high productivity on the Arctic Shelf and in the frontal region during our study. Phytoplankton blooms in the Arctic are restricted to the short ice-free season (Sakshaug, 2004) and productivity in the marginal ice-zone is then temporally high on shelves (Sakshaug, 2004) and in the stabilized marginal ice-zone in general (Carmack and Wassmann, 2006). The biovolume spectra collected here thus agree well with expectations and demonstrate a straightforward way to use the towed LOPC in combination with a CTD for quickly assessing spatial and temporal distributions of physical and biological variables prevailing in the study area during sampling.

Intercepts of the biovolume spectra from the end of April in Atlantic Water resembled the low intercepts of biovolume spectra observed in December in the Barents Sea south of Bjørnøya (Bear Island) (Zhou *et al.*, 2009) and thus further confirm that the zooplankton community in Atlantic Water was still in a winter situation. By mid-May, intercepts in Atlantic Water had slightly increased, indicating that a pre-bloom situation may have developed in parts of the Atlantic Water. This corresponds well to the observed slightly higher fluorescence values in the southeastern-most part of the study area on 15 May.

The number of TLs within the zooplankton community increased in Arctic Water from 3.6 to 5.5, following the apparent development of the phytoplankton bloom. Top predators within the zooplankton community in Arctic Water were chaetognaths, amphipods (mostly *Parathemisto libellula*) and ctenophores. A TL of 3.6 agrees well with TLs determined by stable isotope analyses for these carnivores in spring (Søreide *et al.*, 2006), and indicates the dominance of a classic food chain where phytoplankton is ingested by *Pseudocalanus* spp. and *Calanus* spp., and these in turn are ingested by

carnivorous zooplankton. For older stages of *C. glacialis* and *C. finmarchicus*, which clearly dominated the large zooplankton size group in Arctic Water, TL increased from 2.2 to 4.4 at the end of the sampling. This indicates that *Calanus* spp. fed nearly exclusively as a herbivore during the bloom, while phytoplankton biomass likely was channelled through the microbial loop, e.g. via flagellates and ciliates, late in the bloom. This is consistent with an observed increase in the number of trophic links between microzooplankton and *Calanus* as the phytoplankton bloom progresses (Levinsen *et al.*, 2000) and corresponds also well with an observed increase in TL of *C. glacialis* with the progression of the bloom (Tamelander *et al.*, 2008). The higher number of TLs within the zooplankton community at the end of sampling in Arctic Water may then reflect that carnivorous zooplankton ingested copepods that had derived their energy from omnivorous diets.

In Polar Front Water, TLs computed by biovolume spectrum theory gave contradictory results: At the end of April, the maximum number of TLs within the zooplankton community was 3.9, while a TL of 5.5 was computed for the large zooplankton group (*Calanus* or possibly juvenile krill) alone. This can be understood as follows: computing TLs according to biovolume spectrum theory is based on the assumption that the biovolume spectrum can be linearized on a logarithmic scale (Zhou, 2006). We only computed TLs for significant slopes so as not to violate this assumption; however, looking at the biovolume spectra from Polar Front Water (Fig. 5), cycling deviations from the fitted line are obvious. Hence, a significant fit of the regression line was obtained, in spite of a non-linear biovolume spectrum. For Polar Front Water, and to a lesser degree also for Atlantic Water, the TLs computed for the whole zooplankton community thus have to be viewed as mean trophic values within the community, rather than as the maximum number of TLs within the zooplankton community. No deviations from a linear logarithmic biovolume spectrum were observed in the medium and large zooplankton size groups, and thus for these groups, a maximum TL could be computed.

Before the bloom reached Polar Front Water, older stages of *Calanus* spp. had a high TL reflecting an omnivorous diet. Later on, the TL decreased to 3.1, likely reflecting a more herbivorous diet in *Calanus*, as was observed in Arctic Water in the beginning of the bloom. Possibly also an increased abundance of juvenile, mostly herbivorous *Thysanoessa* spp. (Søreide *et al.*, 2006) contributed to the decrease in TL in the large zooplankton group. Within the whole zooplankton community, mean TL increased towards the mid of May. This might be attributed to the large patch of XL zooplankton, which was observed in the study area then. We cannot say with certainty if this patch consisted of euphausids or not, but regard it as likely based on (i) net samples showing krill larvae and (ii) the observed distribution in the Polar Front, which is typical for *Thysanoessa* spp. (Dalpadado and Skjoldal, 1996). Older stages of *T. inermis* and *T. longicaudata* are omnivorous to a variable degree (Falk-Petersen *et al.*, 2000; Søreide *et al.*, 2006; Dalpadado *et al.*, 2008) and thus have the potential to increase mean TL within the zooplankton community.

In all water masses, surprisingly low TLs between 1.0 and 1.2 were computed at the end of April for the medium-sized zooplankton group, which mostly consisted of *Pseudocalanus* spp. These low TLs indicate that TLs were underestimated in the medium zooplankton group. Assimilation efficiency was assumed to be 70%, but might have been lower in *Pseudocalanus* spp., as was discussed in the Method section. Assuming an assimilation efficiency of 50% would increase TL by 0.2. Independent of assimilation efficiency, the very low TLs computed for the medium-sized zooplankton group indicate that *Pseudocalanus* spp. fed mostly herbivorously.

The prevailing winter situation in Atlantic Water becomes clear when looking at TLs. The number of TLs in the zooplankton community was high at the beginning of the study, reflecting a community in which biomass is being recycled several times. The few large zooplankton found in the upper layer (*C. finmarchicus*) had a high TL of 5.6, similar to the TL in the late bloom/post bloom situation in Arctic Water. Later on, mean TL in the whole zooplankton community decreased, likely due to an increase in herbivorous *Balanus* sp. nauplii (Turner *et al.*, 2001) in the upper layer. Also the TL in the large zooplankton group decreased with time, and this probably shows the ascent of the first *C. finmarchicus* from overwintering depths, which then started feeding on phytoplankton.

Trophic structure within the pelagic community was thus highly variable across the Polar Front. The variability was closely related to the stage of the phytoplankton bloom with generally higher TLs outside bloom situations, likely due to (i) increased abundances of herbivorous meroplanktonic larvae during the bloom and (ii) increased omnivory of *Calanus* spp. during pre- and post-bloom. Estimating TLs based on biovolume spectrum theory is a new approach (Zhou, 2006) that has not been extensively tested using field data. As has been shown in this study, it yields reasonable values for TLs within the zooplankton community as long as the underlying assumptions are met. Applying biovolume spectrum theory to data collected by semi-automatic sampling proved thus to be a powerful method to analyse the effect of mesoscale hydrography on trophic

dynamics within the pelagic community, not at least in a dynamic frontal area. In the future, it would be desirable to combine the estimation of TLs using biovolume spectrum theory with methods that determine TLs based on direct sampling of a variety of planktonic organisms, e.g. stable isotope analyses. This would allow direct comparison of TL estimates from both methods for different groups of zooplankon, namely herbivores, omnivores and carnivores, and thus to obtain a greater certainty that estimated TLs reliably describe the trophic interactions within the zooplankton community.

It has to be noted that detritus is incorporated into the estimation of TLs when using biovolume spectrum theory. This leads to higher TLs compared with approaches where detritus is assigned TL one (Pauly *et al.*, 1998), or where the background level of the food web (TL one) is determined based on particulate organic matter that includes detritus and phytoplankton alike, as is common in stable isotope analyses of marine pelagic food webs (Hobson *et al.*, 1995; Søreide *et al.*, 2006). It is complex to define the first TL in food webs (Post, 2002), especially for systems with many omnivorous species (Williams and Martinez, 2004) and a high variability on spatial scales (Tamelander *et al.*, 2009), such as the pelagic system. It is debatable whether it is feasible to include detritus into the food web or not. On the one hand, detritus is important for the flow of energy within food webs (Moore *et al.*, 2004), on the other hand food chains may become impractically long leading to very high TLs (Williams and Martinez, 2004). In the euphotic zone, detritus forms a vital source of energy for many organisms and is thus recycled frequently (Wexels Riser *et al.*, 2007). When addressing the trophic linkages within the zooplankton community, we therefore think that incorporating detritus into the food web gives a more complete view of the trophic situation than levelling detritus to TL one.

ACKNOWLEDGEMENTS

We thank Malin Daase for quick and thorough processing of the zooplankton samples, John Terje Eilertsen and Richard Buvang for excellent technical assistance during the cruise, Ken Drinkwater for ample sampling time and a friendly atmosphere during the cruise and Tobias Tamelander for inspiring discussions.

FUNDING

This work was supported by the Research Council of Norway as part of the NESSAR project [# 176057/S30]. Funding to pay the Open Access publication charges for this article was provided by the Centre for Gender Research at the University of Tromsø.

REFERENCES

Anonymous (2006) *LOPC Software Operation Manual*. Brooke Ocean Technology Ltd, Dartmouth, Nova Scotia, Canada.

Basedow, S. L. and Tande, K. S. (2006) Cannibalism by female *Calanus finmarchicus* on naupliar stages. *Mar. Ecol. Prog. Ser.*, **327**, 247–255.

Basedow, S. L., Edvardsen, A. and Tande, K. S. (2008) Vertical segregation of *Calanus finmarchicus* copepodites during the spring bloom. *J. Mar. Syst.*, **70**, 21–32.

Blachowiak-Samolyk, K., Kwasniewski, S., Dmoch, K. *et al.* (2007) Trophic structure of zooplankton in the Fram Strait in spring and autumn 2003. *Deep-Sea Res. II*, **54**, 2716–2728.

Carmack, E. and Wassmann, W. (2006) Food webs and physical–biological coupling on pan-Arctic shelves: unifying concepts and comprehensive perspectives. *Prog. Oceanogr.*, **7**, 446–477.

Corkett, C. J. and McLaren, I. A. (1978) Biology of *Pseudocalanus*. *Adv. Mar. Biol.*, **15**, 1–231.

Daase, M. and Eiane, K. (2007) Mesozooplankton distribution in northern Svalbard waters in relation to hydrography. *Polar Biol.*, **30**, 969–981.

Dalpadado, P. and Skjoldal, H. R. (1996) Abundance, maturity and growth of the krill species *Thysanoessa intermis* and *T. longicaudata* in the Barents Sea. *Mar. Ecol. Prog. Ser.*, **144**, 175–183.

Dalpadado, P., Yamaguchi, A., Ellertsen, B. *et al.* (2008) Trophic interactions of macro-zooplankton (krill and amphipods) in the Marginal Ice Zone of the Barents Sea. *Deep-Sea Res. II*, **55**, 2266–2274.

Edvardsen, A., Zhou, M., Tande, K. *et al.* (2002) Zooplankton population dynamics: measuring *in situ* growth and mortality rates using an Optical Plankton Counter. *Mar. Ecol. Prog. Ser.*, **227**, 205–219.

Eilertsen, H. C. (1993) Spring blooms and stratification. *Nature*, **363**, 24.

Engelsen, O., Hegseth, E. N., Hop, H. *et al.* (2002) Spatial variability of chlorophyll-*a* in the Marginal Ice Zone of the Barents Sea, with relations to sea ice and oceanographic conditions. *J. Mar. Syst.*, **35**, 79–97.

Falk-Petersen, S., Hagen, W., Kattner, G. *et al.* (2000) Lipids, trophic relationships and biodiversity in Arctic and Antarctic krill. *Can. J. Fish. Aquat. Sci.*, **57**, 178–191.

Fenchel, T. (2008) The microbial loop—25 years later. *J. Exp. Mar. Biol. Ecol.*, **366**, 99–103.

Gaardsted, F., Tande, K. S. and Basedow, S. L. Measuring copepod abundance in deep water winter habitats in the NE Norwegian Sea: intercomparison of results from laser optical plankton counter and multinet. *Fish. Oceanogr.*, in review

Gallienne, C. P. and Robins, D. B. (2001) Is *Oithona* the most important copepod in the world's oceans? *J. Plankton Res.*, **23**, 1421–1432.

Harris, R. P. and Paffenhöfer, G. A. (1976) Effect of food concentration on cumulative ingestion and growth efficiency of 2 small marine planktonic copepods. *J. Mar. Biol. Assoc. UK*, **56**, 875–888.

Heath, M. R. (1995) Size spectrum dynamics and the planktonic ecosystem of Loch Linnhe. *ICES J. Mar. Sci*, **52**, 627–642.

Herman, A. W., Beanlands, B. and Phillips, F. (2004) The next generation of Optical Plankton Counter: the Laser-OPC. *J. Plankton Res.*, **26**, 1135–1145.

Hobson, K. A., Ambrose, W. G. and Renaud, P. E. (1995) Sources of primary production, benthic–pelagic coupling, and trophic relationships within the Northeast Water Polynya: insights from C and N analysis. *Mar. Ecol. Prog. Ser.*, **128**, 1–10.

Hodal, H. and Kristiansen, S. (2008) The importance of small-celled phytoplankton in spring blooms at the marginal ice zone in the northern Barents Sea. *Deep-Sea Res. II*, **55**, 2176–2185.

Hunter, J. D. (2007) Matplotlib: a 2D Graphics Environment. *Comput. Sci. Eng*, **9**, 90–95. http://matplotlib.sourceforge.net/.

Kirchmann, D. L. (ed.) (2000) *Microbial Ecology of the Oceans. Ecol. Appl. Microbiol.*, Wiley-Liss, New York, pp. 542.

Koski, M., Breteler, W. K. and Schogt, N. (1998) Effect of food quality on rate of growth and development of the pelagic copepod *Pseudocalanus elongatus* (Copepoda, Calanoida). *Mar. Ecol. Prog. Ser.*, **170**, 169–187.

Lang, W. H. and Ackenhusen-Johns, A. (1981) Seasonal species composition of barnacle larvae (Cirripedia: Thoracica) in Rhode Island waters, 1977–1978. *J. Plankton Res.*, **3**, 567–575.

Law, R., Plank, M. J., James, A. *et al.* (2009) Size-spectra dynamics from stochastic predation and growth of individuals. *Ecology*, **90**, 802–811.

Levinsen, H., Turner, J. T., Nielsen, T. G. *et al.* (2000) On the trophic coupling between protists and copepods in arctic marine ecosystems. *Mar. Ecol. Prog. Ser.*, **204**, 65–77.

Loeng, H. (1991) Features of the physical oceanographic conditions in the Barents Sea. *Polar Res.*, **10**, 5–18.

Mauchline, J. (1998) The biology of calanoid copepods. *Adv. Mar. Biol.*, **33**, 1–710.

Moore, J. C., Berlow, E. L., Coleman, D. C. *et al.* (2004) Detritus, trophic dynamics and biodiversity. *Ecol. Lett.*, **7**, 584–600.

Nichols, J. H. and Thompson, A. B. (1991) Mesh selection of copepodite and nauplius stages of four calanoid copepod species. *J. Plankton Res.*, **13**, 661–671.

Pauly, D., Christensen, V., Dalsgaard, J. *et al.* (1998) Fishing down marine food webs. *Science*, **279**, 860–863.

Platt, T. and Denman, K. (1977) Organization in the pelagic ecosystem. *Helgoländer wiss. Meeresunters*, **30**, 575–581.

Platt, T. and Denman, K. (1978) The structure of pelagic marine ecosystems. *Rapp. P.-V. Réun. Cons. Int. Explor. Mer*, **173**, 60–65.

Post, D. M. (2002) Using stable isotopes to estimate trophic position: models, methods, and assumptions. *Ecology*, **83**, 703–718.

Quinones, R. A., Platt, T. and Rodríguez, J. (2003) Patterns of biomass-size spectra from oligotropic waters of the Northwest Atlantic. *Prog. Oceanogr*, **57**, 405–427.

Reigstad, M., Wassmann, P., Wexels Riser, C. *et al.* (2002) Variations in hydrography, nutrients and chlorophyll *a* in the marginal ice-zone and the central Barents Sea. *J. Mar. Syst.*, **38**, 9–29.

Rey, F. and Loeng, H. (1985) The influence of ice and hydrographic conditions on the development of stress on marine organism. In Gray, J. S. and Christiansen, M. E. (eds), *Marine Biology of Polar Regions and Effect of Stress on Marine Organism*. John Wiley & Sons Ltd, Chichester, pp. 49–63.

Rey, F., Skjoldal, H. R. and Slagstad, D. (1987) Primary production in relation to climatic changes in the Barents Sea. In Loeng, H. (ed.), *The Effect of Oceanographic Conditions on Distribution and Population Dynamics of Commercial Fish Stocks in the Barents Sea. Proceedings of the 3rd Soviet-Norwegian Symposium*. Institute of Marine Research, Bergen, pp. 9–46.

Sakshaug, E. (2004) Primary and secondary production in the Arctic seas. In Stein, R. and Macdonald, R. W. (eds), *The Organic Carbon Cycle in the Arctic Ocean*. Springer Verlag, Berlin, pp. 57–81.

Sameoto, D., Wiebe, P., Runge, J. *et al.* (2000) Collecting zooplankton. In Harris, R. P., Wiebe, P. H., Lenz, J. *et al.* (eds), *ICES Zooplankton Methodology Manual*. Academic Press, London, pp. 59–81.

Signorini, S. R. and McClain, C. R. (2009) Environmental factors controlling the Barents Sea spring–summer phytoplankton blooms. *Geophys. Res. Lett.*, **36**, l10604.

Silvert, W. and Platt, T. (1978) Energy flux in the pelagic ecosystem: a time-dependent equation. *Limnol. Oceanogr.*, **23**, 813–816.

Søreide, J. E., Hop, H., Carroll, M. L. *et al.* (2006) Seasonal food web structures and sympagic–pelagic coupling in the European Arctic revealed by stable isotopes and a two-source food web model. *Prog. Oceanogr.*, **71**, 59–87.

Sprules, W. G. and Munawar, M. (1986) Plankton size spectra in relation to ecosystem productivity, size and perturbation. *Can. J. Fish. Aquat. Sci*, **43**, 1789–1794.

Tamelander, T., Reigstad, M., Hop, H. *et al.* (2008) Pelagic and sympagic contribution of organic matter to zooplankton and vertical export in the Barents Sea marginal ice zone. *Deep-Sea Res. II*, **55**, 2330–2339.

Tamelander, T., Kivimäe, C., Bellerby, R. G. J. *et al.* (2009) Base-line variations in stable isotope values in an Arctic marine ecosystem: effects of carbon and nitrogen uptake by phytoplankton. *Hydrobiology*, **630**, 63–73.

Turner, J. T., Levinsen, H., Nielsen, T. G. *et al.* (2001) Zooplankton feeding ecology: grazing on phytoplankton and predation on protozoans by copepod and barnacle nauplii in Disko Bay, West Greenland. *Mar. Ecol. Prog. Ser.*, **221**, 209–219.

von Quillfeldt, C. (2000) Common diatom species in arctic spring blooms: their distribution and abundance. *Bot. Mar.*, **43**, 499–516.

Waniek, J. J., Holliday, N. P., Davidson, R. *et al.* (2005) Freshwater control of onset and species composition of Greenland shelf spring bloom. *Mar. Ecol. Prog. Ser.*, **288**, 45–47.

Wassmann, P., Ratkova, T., Andreassen, I. *et al.* (1999) Spring bloom dynamics in the marginal ice zone and the central Barents Sea. *Mar. Ecol. PZNI*, **20**, 321–346.

Wexels Riser, C., Reigstad, M., Wassmann, P. *et al.* (2007) Export or retention? Copepod abundance, faecal pellet production and vertical flux in the marginal ice zone through snap shots from the northern Barents Sea. *Polar Biol.*, **30**, 719–730.

Williams, R. J. and Martinez, N. D. (2004) Limits to trophic levels and omnivory in complex food webs: theory and data. *Am. Nat.*, **163**, 458–468.

Zhou, M. (2006) What determines the slope of a plankton biomass spectrum? *J. Plankton Res.*, **28**, 437–448.

Zhou, M. and Huntley, M. (1997) Population dynamics theory of plankton based on biomass spectra. *Mar. Ecol. Prog. Ser.*, **159**, 61–73.

Zhou, M., Zhu, Y. and Peterson, J. (2004) *In situ* growth and mortality of mesozooplankton during the austral fall and winter in Marguerite Bay and its vicinity. *Deep-Sea Res. II*, **51**, 2099–2118.

Zhou, M., Tande, K. S., Zhu, Y. *et al.* (2009) Productivity, trophic levels and size spectra of zooplankton in northern Norwegian shelf regions. *Deep-Sea Res. II*, doi:10.1016/j.dsr2.2008.11.018.